Importance of Matching Physical Friction, Hardness, and Texture in Creating Realistic Haptic Virtual Surfaces

Heather Culbertson, *Member, IEEE* and Katherine J. Kuchenbecker, *Member, IEEE*

Abstract—Interacting with physical objects through a tool elicits tactile and kinesthetic sensations that comprise your haptic impression of the object. These cues, however, are largely missing from interactions with virtual objects, yielding an unrealistic user experience. This article evaluates the realism of virtual surfaces rendered using haptic models constructed from data recorded during interactions with real surfaces. The models include three components: surface friction, tapping transients, and texture vibrations. We render the virtual surfaces on a SensAble Phantom Omni haptic interface augmented with a Tactile Labs Haptuator for vibration output. We conducted a human-subject study to assess the realism of these virtual surfaces and the importance of the three model components. Following a perceptual discrepancy paradigm, subjects compared each of 15 real surfaces to a full rendering of the same surface plus versions missing each model component. The realism improvement achieved by including friction, tapping, or texture in the rendering was found to directly relate to the intensity of the surface's property in that domain (slipperiness, hardness, or roughness). A subsequent analysis of forces and vibrations measured during interactions with virtual surfaces indicated that the Omni's inherent mechanical properties corrupted the user's haptic experience, decreasing realism of the virtual surface.

Index Terms—Virtual reality, data-driven modeling, high-frequency vibrations, haptic texture rendering, force feedback

1 Introduction

The sensations you feel when interacting with the physical world through a tool are rich and varied. For example, if you pick up a stylus and gently drag its tip across a rock or a swatch of leather, you can feel variations in the friction and texture even though your fingers are not directly touching the surface. Pressing the tool into different surfaces provides information about surface deformation, and tapping elicits transient vibrations that convey surface hardness [1]. Interestingly, the mechanical interaction strongly depends on both the properties of the surface and how you move the tool. The human sense of touch excels at sensing and interpreting the signals that are generated by the contacts and transmitted through the tool [2], giving you a clear impression of the surface.

The field of haptic rendering seeks to understand the sensations felt during physical interactions to create realistic virtual objects that can be felt as well as seen. Traditional haptic rendering algorithms and devices, however, cannot output high-fidelity reproductions of surface contacts [3], [4]. Surfaces are commonly represented using a Hooke's law relationship with output force proportional to the user's penetration into the object. The maximum stiffness an impedance-type haptic device can stably render is limited by the system's sampling rate, computation time, and quantization [4], [5]. These limitations cause hard virtual objects to feel unrealistically soft and spongy. The motor drive circuitry [6] and friction and flexibility in the device [3] limit its ability to accurately reproduce high-frequency vibrations, meaning that virtual surfaces often do not include texture and thus feel smooth and slippery. Physics-based simulations of textured surfaces are too computationally intensive for real-time haptic rendering [7], [8].

To overcome the limitations of physics-based simulation, many researchers have sought to capture the complexities of physical interactions using data recorded during the real interaction of interest [9]. These data-driven modeling methods have shown promise in creating realistic virtual sensations, but most focus on modeling only one component of the surface, as summarized in Section 2. For example, we have created virtual haptic textures by modeling and rendering the high-frequency vibrations that result from dragging a tool across textured surfaces [10], [11], [12], [13], [14]. A human subject study showed that these vibrations accurately presented the roughness information of the surface, but they did not capture any of its slipperiness information and did not completely capture its hardness [13]. This result indicated that other modeling and rendering components are necessary to fully capture and recreate the haptic sensations felt when touching surfaces with a tool.

This article evaluates our efforts to render highly realistic virtual surfaces by expanding our past work in texture rendering to include surface friction and tapping transients.

- *H. Culbertson is with the Department of Mechanical Engineering and Applied Mechanics, University of Pennsylvania, Philadelphia, PA 19104. E-mail: hculb@seas.upenn.edu.*
- *K.J. Kuchenbecker is with the Department of Mechanical Engineering and Applied Mechanics, and the Department of Computer and Information Science, University of Pennsylvania, Philadelphia, PA 19104. E-mail: kuchenbe@seas.upenn.edu.*

Manuscript received 28 Mar. 2016; revised 7 July 2016; accepted 27 July 2016. Date of publication 10 Aug. 2016; date of current version 16 Mar. 2017. Recommended for acceptance by C. Duriez.
For information on obtaining reprints of this article, please send e-mail to: reprints@ieee.org, and reference the Digital Object Identifier below.
Digital Object Identifier no. 10.1109/TOH.2016.2598751

Section 3 summarizes our haptic surface modeling and rendering methods. As described in Section 4, we designed and ran a human-subject study to evaluate the improvements in realism that can be achieved by adding friction, tapping, and texture cues to 15 different virtual surfaces. This study assessed the contribution of the three components of the haptic surface model and determined whether all three model components are needed to create realistic virtual versions of each surface. The results of the study are presented in Section 5 and discussed in Section 6. Section 7 summarizes the results and conclusions of this article.

2 Background

Traditional rendering schemes cannot fully capture the haptic sensations one experiences when touching physical objects. These rendering algorithms typically present the shape of objects, but they are missing other important haptic cues. When contacted through a tool, objects can be characterized by three main perceptual components: slipperiness, hardness, and roughness [15]. To capture these three perceptual dimensions, researchers have sought ways to accurately model and render surface friction, tapping behavior, surface stiffness, and texture vibrations. Yamauchi et al. [16] and McMahan et al. [17] both created systems to sense and directly communicate these material properties from slave to master in teleoperation. Haptic rendering schemes, however, must model the haptic signals through a simplification of the underlying physics in order to store the interactions for use in later real-time rendering. To create virtual haptic interactions that feel realistic, many researchers have implemented data-driven methods, which seek to capture the output response of a system given user inputs [9]. Past work in haptic modeling and rendering has tended to focus on capturing only one perceptual dimension, but slipperiness, hardness, and roughness are all important in creating the full perceptual feel of the surface.

2.1 Friction

The perceptual dimension of slipperiness has been found to originate from surface friction [15]. Kinetic friction is modeled as the tangential force that resists motion when a tool is dragged across a surface with a certain normal force and tangential speed. In addition, some friction models include a region of static friction, which resists the start of motion. Several friction modeling techniques of differing complexity have been explored for use in haptic rendering. Richard et al. presented a method for modeling the friction between an aluminum block and surface materials from measured force, acceleration, and velocity data [18]. Worden et al. also explored modeling pre-sliding and sliding friction using data that were recorded using a tribometer [19]. Jeon et al. fit force, position, and velocity data to a Dahl friction model, which was then used to render friction in a haptic augmented reality scheme [20]. Since the behavior of the surface friction varies greatly depending on the properties of the two surfaces in sliding contact, an appropriate friction model must be chosen by observing the behavior of the individual system. During rendering, friction is typically displayed to the user through a force-feedback haptic device. However the importance of friction in rendering virtual surfaces has not been previously examined.

2.2 Tapping Transients

Researchers have long known that perceptual hardness in bare-finger interactions depends on the elasticity or compressibility of the surface [15]. In contrast, LaMotte's study of tool-based interactions found that humans were significantly better at discriminating the hardness of surfaces when tapping rather than when pressing into the surface [1]. This result indicates that the transient vibrations elicited by tapping a tool largely determine the surface's perceived hardness and can be used to change the perceived hardness of a virtual surface.

Methods for modeling these transient signals typically follow either an input-output or database approach [9]. In an input-output approach, a mathematical relationship is found between the system parameters (e.g., material type, velocity) and the system's output (e.g., measured vibrations). Wellman and Howe approximated the force response of a stylus tapped on a rigid surface as an exponentially decaying sinusoid with a frequency and amplitude that depend on the material and the impact velocity [21]. Okamura et al. extended this work by creating a library of tapping responses for multiple materials, showing that the frequency of the tap increased with surface stiffness [22]. Their study indicated that subjects were able to discriminate between hardnesses of virtual surfaces using either a combination of force and tapping vibration feedback or vibration feedback alone. In a database approach, a set of transient vibration signals are recorded from repeated taps on the surface and are stored directly. Kuchenbecker et al. [4] compared the realism of virtual surfaces using a database approach, an input-output approach, and Hooke's law. The study showed that overlaying either the recorded acceleration transients or manually tuned and velocity-scaled decaying sinusoids on a virtual surface resulted in a perceived hardness that closely matched that of a real surface.

2.3 Texture

The perceptual roughness of surfaces felt through a tool is known to depend on the vibrations induced during dragging [23], [24], [25], [26]. Several researchers have explored modeling these vibrations to create virtual haptic textures. Okamura et al. [22] represented patterned textures as a set of data-driven decaying sinusoids at the material's characteristic frequency. These textures were rendered and displayed to users through a force-feedback device. Guruswamy et al. [27] took a similar approach and created texture models based on a spatial distribution of infinite-impulse-response filters that are fit with decaying sinusoids. Lang and Andrews [28] modeled textures as height profiles using accelerations measured while dragging a handheld tool across a surface. Our past work has modeled texture vibrations as an autoregressive process that depends on the user's force and speed [10], [11], [12], [13], [14], [29]. Other researchers have created virtual textures by directly playing back recorded vibrations though a voice-coil actuator [30] and a cable-driven haptic interface [31]. While simple, directly playing back the recorded texture vibrations cannot capture how tool force and speed affect the vibrations. Past work has shown that virtual textures must respond to changing interaction conditions in order to be realistic [32].

3 Surface Modeling and Rendering

The haptic surface models presented in this article are composed of three separate components: surface friction, tapping transients, and texture vibrations. These components seek to capture the surface's perceptual slipperiness, hardness, and roughness, respectively. We create each component model using data recorded from interactions between a handheld tool and the real surface. This Section summarizes the recording, data processing, and modeling procedures that we use to build the three component models for a given surface, as well as methods for rendering these models to create the virtual surface using a SensAble Phantom Omni augmented with a voicecoil actuator. These modeling and rendering methods are adapted from [4], [13], [33].

3.1 Recording Hardware

To create realistic data-driven haptic virtual surfaces, we must use recording hardware that is as mechanically similar as possible to the rendering hardware. This similarity is necessary because the vibration generation and transmission to the user's fingertips depend on the entire tool-hand-surface system. Although the virtual surfaces are rendered using an Omni, it was not suitable to record data using sensors attached to the Omni because its internal drivetrain creates additional forces and vibrations that would contaminate the surface recording and decrease the realism of the models. We instead use our previously-created custom handheld device to record the tip speed, contact force, and high-frequency acceleration of a tool as it interacts with physical surfaces [12], [14]. An Ascension 3D Guidance TrakSTAR magnetic tracking sensor, which is embedded in the back of the tool, measures the tool's position and orientation at 240 Hz with resolutions of 0.5 mm and 0.1 degree, respectively. A six-axis force-torque sensor (ATI Industrial Automation Nano17 SI-25-0.25) is located between the tooltip and the body of the tool. A 3.175-mm-diameter stainless steel hemispherical tooltip is attached to the force sensor for surface interaction. Two ± 18 g two-axis accelerometers (Analog Devices ADXL321) are rigidly embedded in the body of the tool orthogonal to one another.

The signals output by the force sensor and the accelerometers are read into an analog-to-digital DAQ device (National Instruments USB-6259) at 10 kHz. The accelerations are low-pass filtered at 1,000 Hz with an analog five-pole Bessel filter to remove effects of sensor resonance. The three recorded acceleration signals from the sensor's three axes were mapped onto a single axis using the DFT321 algorithm presented in [34], which preserves the spectral and temporal properties of the three-axis signals. This mapping is possible because humans cannot determine the direction of vibrations at high frequencies [35]. The combined acceleration was high-pass filtered at 20 Hz to remove the effects of gravity and purposeful human motion. The recorded data is used to create haptic models of the surface's friction, tapping transients, and texture.

3.2 Rendering the Base Surface

Friction, tapping, and texture are overlaid on a virtual base surface that is rendered using the Omni, which measures the user's position and outputs a force. When the user is touching the surface, the haptic device's endpoint is referred to as the Haptic Interface Point (HIP), and the corresponding point on the surface is referred to as the Ideal Haptic Interface Point (IHIP) [36]. The virtual base surface is displayed using a Hooke's law relationship so the normal force is proportional to the user's penetration depth into the surface ($y \equiv$ the distance between the HIP and the IHIP) with a stiffness of $k = 0.25$ N/mm. This stiffness was chosen to give all surfaces the same underlying stiffness; the perceived hardness was changed by the tapping transients alone. A higher stiffness left the softer surfaces feeling too hard. Furthermore, we wanted subjects to use a wide range of normal forces. Because of the Hooke's law relationship, the force resolution is proportional to the Omni's position resolution. When the stiffness value is high, only a small penetration depth is needed to reach the maximum force, making it difficult for users to apply small forces.

3.3 Haptic Surface Components

To match the complexity of real surfaces, we modeled surface friction, tapping transients, and texture vibrations for each surface from recorded data. During rendering, the models are used to generate force and vibration signals that are added to the forces generated by the base surface before being rendered to the user.

3.3.1 Friction

Friction Data Recording: The experimenter dragged the tool across the chosen physical surface in a continuous circular motion while ten seconds of the tool's position, orientation, and force were recorded using the sensors described above. The three axes of force data were downsampled to 240 Hz and were then separated into their tangential and normal components. The recordings used to make the friction models in this article are the same as those available in our open-source Penn Haptic Texture Toolkit (HaTT) [37].

Friction Model Creation: In this article, we implement a Dahl friction model, which was first presented in [38] and adapted for use in haptic rendering by Hayward et al. [33]. The Dahl friction model represents friction as quasi-static contact bonds that are continuously formed and then broken, beneficially accounting for static friction and the transition to sliding motion. We found that the simplest version of Dahl friction for sliding objects, the stick-slip model, was appropriate for modeling the friction between the recording tool and the surfaces modeled in this article. The stick-slip model has a region of presliding displacement (static friction) followed by sliding contact with simple Coulomb friction (kinetic friction).

Coulomb friction dictates that the tangential friction force F_f is proportional to the normal force F_n via $F_f = \mu_k F_n$. A line through the origin was fit to the plot of the recorded tangential versus normal force, and the slope of the line is the kinetic friction coefficient, μ_k.

Friction Rendering: In the stick-slip Dahl friction model, the HIP x and IHIP w are connected by a virtual spring. The first stage of spring stretch represents the presliding stick shown in Fig. 1. The second stage of spring stretch, the sliding region, follows simple Coulomb friction. The location of the adhesion point on the surface is calculated as

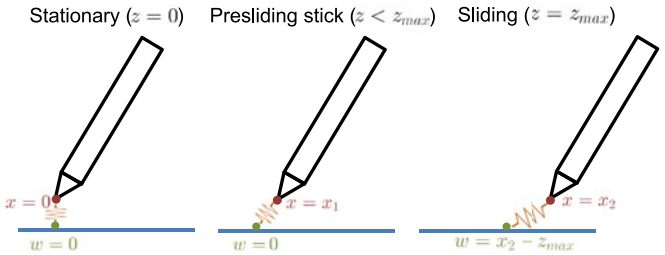

Fig. 1. Representation of a tool dragging along a surface in the Dahl friction model. The tool and a point on the surface are modeled as being connected by a spring.

$$w_i = \begin{cases} x_i - \text{sign}(x_i - x_{i-1}) z_{\max} & \text{if } |x_i - w_{i-1}| > z_{\max} \\ w_{i-1} & \text{otherwise,} \end{cases} \quad (1)$$

where w_{i-1} is the previous location of the adhesion point, x_i is the current location of the tool, and x_{i-1} is the previous location of the tool. The friction force is then calculated as

$$\begin{aligned} z_i &= x_i - w_i \\ F_f &= \mu_k F_n \left(\frac{z_i}{z_{\max}} \right), \end{aligned} \quad (2)$$

where the normal force is calculated using constant stiffness ($F_n = k \cdot y$). The friction force is oriented to oppose the occurring tangential velocity.

For our system, we empirically tuned the Dahl friction model to choose the value of $z_{\max}$ which would ensure stability of the system. Surfaces with higher friction required a larger value for $z_{\max}$ than surfaces with low friction, leading us to choose $z_{\max}$ to be proportional to the kinetic friction coefficient ($z_{\max} = 4 \text{ mm} \cdot \mu_k$). Although this empirical value for $z_{\max}$ does not correctly capture the interaction's static friction, we compromised on accuracy to ensure the stability of the haptic rendering.

3.3.2 Tapping Transients

Tapping Data Recording: The tapping model presented in this article is adapted from the event-based feedback presented in [4]. Ten seconds of position, force, and acceleration data were recorded while the experimenter tapped on the selected surface using the recording device. The experimenter varied the speed at which the contact occurred to capture a wide range of incoming speeds during each recording.

The magnetic tracking sensor's position and orientation measurements were upsampled to 10 kHz and used to calculate the position of the tooltip. The speed of the tool just prior to tapping was calculated using the discrete-time derivative of the tooltip position. The speed was low-pass filtered at 100 Hz to suppress noise.

Tapping Model Creation: The combined acceleration signal was manually partitioned into the individual taps, which were aligned temporally. Each tap was labeled with the speed of the tooltip immediately before contact. Following [4], we saved 100 ms of data after contact. Sample sets of taps for two different materials are shown in Fig. 2. The taps from the harder surface (MDF) are of higher frequency and amplitude. The taps from the softer surface (scouring pad) are slower acting and lower power.

Tapping Rendering: During rendering, the displayed tapping response is a function of the user's incoming contact

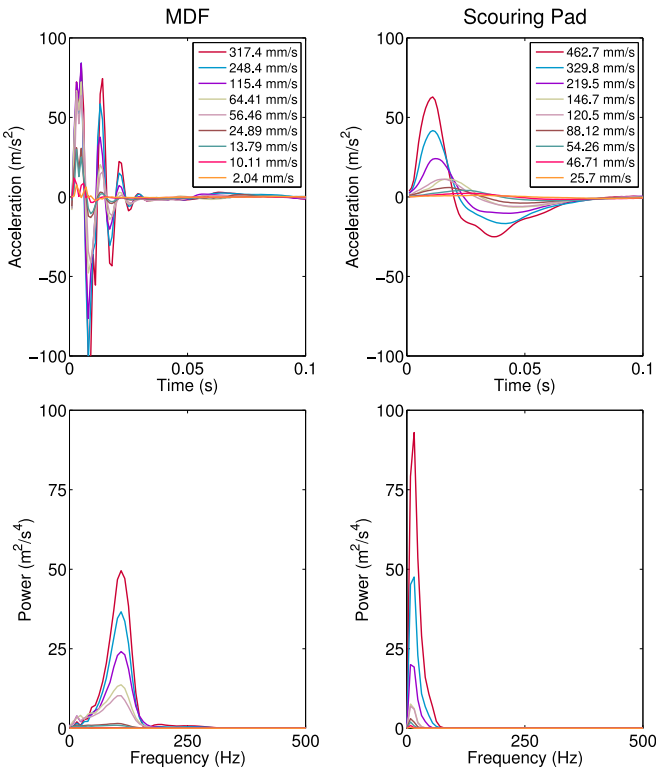

Fig. 2. Recorded tapping transient accelerations for two sample materials. The amplitude of the vibrations depends on the incoming speed of the tool. The spectral content of the vibrations depends on the hardness of the surface.

speed v_{in}, as in [4]. Because the user's mass is constant, the momentum of the Omni-hand system ($p = mv_{\text{in}}$) varies linearly with incoming velocity. Therefore, the amplitude of the transients must also scale with the incoming velocity. This velocity dependence can be seen in the recorded tapping transients in Fig. 2. For incoming speeds lower than the minimum recorded tapping speed, the lowest speed transient is scaled by the quantity $v_{\text{in}}/v_{\min}$. For incoming speeds higher than the maximum tapping speed, the highest speed transient is directly played. For intermediate speeds, the transients from the two bounding speeds are interpolated before being played.

Although the tapping transients are recorded as accelerations, they must be rendered as forces to provide the momentum cancellation necessary to elicit the sensation of tapping on a stiff surface. If the tapping transients are instead played as vibrations, such as through a voice-coil actuator, the user's tool continues to penetrate the surface, creating the sensation of a soft surface. Therefore, the tapping transients are converted to a force through the relationship

$$F_t = m_h a_t, \quad (3)$$

where F_t is the tapping force to be rendered through the Omni, a_t is the desired tapping transient vibration, and m_h is the effective mass of the handle and the user's hand (0.05 kg, as determined in [14]). Although adding the tapping force to the stiffness response momentarily exceeds the maximum steady-state force output of the device, the duration of the high force is sufficiently small (< 0.01 s) not to overheat the motors.

3.3.3 Texture

Our texture modeling and rendering methods were originally presented in [13]. A summary of the data recording and modeling steps are included here for completeness. The texture recordings and models used in this article are available in HaTT [37].

Texture Data Recording: Ten seconds of data were recorded for each texture while the experimenter dragged the recording device along the surface using continuous motions, allowing normal force and scanning speed to vary freely. After the data were recorded, they were processed into measurements of normal force, friction force, tooltip speed, and combined acceleration signal as discussed in [13].

Texture Model Creation: In this article, as in past work [10], [12], [13], [14], [29], we model the acceleration signal using an autoregressive (AR) model structure, which is commonly used in speech processing [39]. Defined by its coefficients and variance, an AR model calculates the system's next output as a linear combination of the previous outputs. The nonstationary behavior of the acceleration signal, which is due to changes in force and speed during recording, requires us to segment the acceleration signal and model it as a piecewise autoregressive process. We create an AR model for each segment and label this model with the median force and median speed used during recording of that segment. The acceleration models are downsampled from 10 kHz to 1 kHz, as in [14], to be compatible with the haptic loop rate required when rendering the textures in a virtual environment created using OpenHaptics and OpenGL.

Texture Rendering: The system generates a texture vibration signal that varies according to the user's interaction conditions in real time. Following [13], measurements of the user's normal force and tangential speed are used to interpolate between models. A white Gaussian excitation signal with power equal to the interpolated variance is generated and used to drive the interpolated model. The excitation signal's history and a history of the previous vibration outputs are used to calculate the new vibration output at a rate of 1,000 Hz.

We output the texture vibrations through a Haptuator voice-coil actuator (Tactile Labs TL-002-14R), which has a bandwidth of 500 Hz. We firmly attached the Haptuator at the tip of the Omni handle using a cable tie, as shown in Fig. 3. The Haptuator must be removed before calibrating the Omni. The texture vibrations are scaled and output through an analog output pin on a Sensoray 626 PCI card at 1,000 Hz. This output voltage is then passed through a linear current amplifier with a gain of 1 A/V to drive the Haptuator.

4 Experimental Methods

This Section describes the human-subject experiment we ran to assess the realism of our haptic virtual surfaces. We also sought to determine the perceptual importance and ecological validity of displaying friction, tapping, and texture information on the virtual surfaces. Described in [40], ecological validity is the correlation between a cue and a property of the world. We wanted to determine how the realism of a virtual surface is affected by the three separate modeling components, and how this relationship depends on the physical surface parameters.

Fig. 3. Experimental set-up. The subject sat at a table in front of a computer and wore headphones playing pink noise to mask auditory cues. The subject used an Omni to feel the virtual surfaces and an adapted Omni handle to feel the real surfaces.

All procedures were approved by the Penn IRB under protocol 820,685. Two separate sets of 15 subjects were recruited for a total of 30 subjects. Twenty-seven subjects were right-handed, and three subjects were left-handed. Twenty-nine subjects had limited experience with haptic devices, and one subject had extensive experience.

4.1 Experimental Setup

The subject sat at a table in front of a computer and wore headphones playing pink noise to mask outside sounds, as shown in Fig. 3. This intervention ensured that the subject used only haptic, and not auditory, cues during the study. The selected virtual surface was represented as a horizontal plane on the screen to match the orientation of the real surfaces. An image of the surface was displayed on the plane, matched to the size of the real surface sample (10×10 cm). A stage was made to hold the real surfaces above the table so the real and virtual surfaces were presented at the same height.

Subjects felt the real surfaces using a detached Omni handle that was modified to have a 3.175-mm-diameter stainless steel hemispherical tooltip to match the tooltip used during data recording. Subjects were instructed to use any motions they desired including dragging, tapping, and pressing into the surface. The experimenter monitored the subject's hand to ensure that it did not contact the surface or the Haptuator. To avoid saturating the motors of the Omni, a visual indicator activated when the normal force exceeded 2.75 N.

4.2 Materials

We wanted this study to use a set of perceptually distinct surfaces to best evaluate the strengths and weaknesses of our surface modeling and rendering approach for surfaces with different friction coefficients, tapping transients, and texture vibrations. Building from the HaTT database of friction and texture models [37], we made a complete set of 100 surface models including friction, tapping transient, and texture components. We chose the surfaces for the study by examining physical properties that correspond to perceived slipperiness, hardness, and roughness.

4.2.1 Surface Property Estimation

The perceived slipperiness of each surface was estimated using the kinetic friction coefficient that resulted from fitting

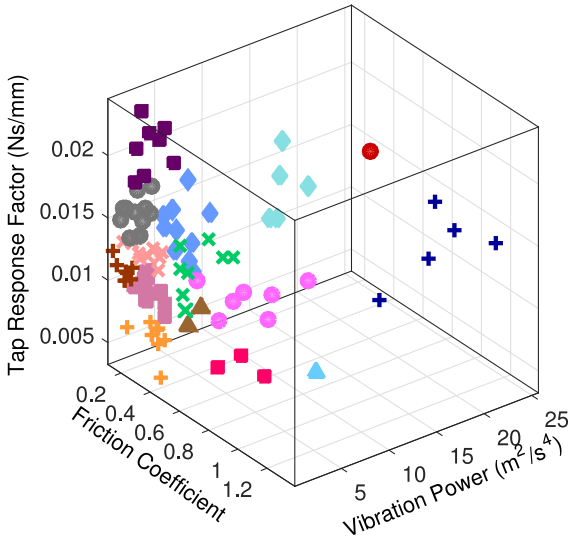

Fig. 4. Clusters of surfaces based on kinetic friction coefficient, tap response factor, and power of texture vibrations. A subset of surfaces that spans the parameter space represented by the original 100 surfaces was chosen by selecting one surface from each cluster.

a Coulomb friction model to the normal and tangential forces recorded as in Section 3.

The perceived hardness of each surface was estimated by fitting a line to a plot of peak normal force at tap versus incoming speed, using the tapping responses described in Section 3. The slope of this line, which we refer to as the tap response factor, was shown to be a valid measure of the primary trend of the dynamics of tapping transients in [41].

We created an indicator for the perceived roughness of the surfaces by synthesizing vibration signals for all 100 textures using a representative force-speed trajectory that spans the area of force-speed space typically explored by humans. The total power of the resulting vibration signal was calculated to represent surface roughness, as in [23], [24], [26], [42].

4.2.2 Surface Clustering

We plotted the 100 surfaces in the three-dimensional space defined by the measurements of friction coefficient, tap response factor, and vibration power, as shown in Fig. 4. To choose a subset of surfaces that are distinct and span the parameter space, we performed hierarchical clustering on the z-scores of the three parameters. An analysis of the scree plot of the Euclidean distances to cluster centroid indicated that about 15 clusters were needed to form distinct groups of surfaces and capture the variation between groups. Fig. 4 shows the resulting clustering for 15 clusters. We wanted the materials to span the parameter space, so we chose one surface from each cluster. The 15 chosen surfaces are shown in Fig. 5.

4.3 Procedure

The study had three phases: adjective ratings of the real surfaces, adjective ratings of the virtual surfaces, and similarity ratings. The first and third phases were completed by one set of 15 subjects, and the second phase was completed by the other set of 15 subjects. The phases were split among two groups of participants to limit the duration of the study.

Fig. 5. The 15 surfaces chosen from the cluster analysis to span the parameter space covered by the original 100 surfaces.

Before the study began, all subjects practiced with the experimental setup and were allowed to feel all of the real surfaces for as long as desired using the tool. Since many subjects were novice haptic users, they were also allowed to practice the motions involved in using the Omni and become familiar with the forces output by the Omni by exploring a simple haptic 3D environment. Study data were collected and managed using Research Electronic Data Capture (REDCap) tools hosted by the University of Pennsylvania [43].

4.3.1 Real Adjective Ratings

The real surfaces were presented to the subject one at a time in randomized order. Subjects rated each surface on the scales of hard-soft, slippery-not slippery and rough-smooth. These scales were chosen from the list provided in [15] as the psychophysical dimensions applicable to the perception of surfaces through a tool. The adjective scales were presented in randomized order, and the subject rated all 15 surfaces on a single scale before moving on to the next scale.

4.3.2 Virtual Adjective Ratings

The procedure described in Section 4.3.1 was completed by a second set of 15 subjects. These subjects rated the 15 virtual surfaces on the same three adjective scales. These virtual surfaces included surface stiffness plus friction, tapping transients, and texture vibrations.

4.3.3 Similarity Ratings

Subjects cannot directly assess the relative importance of the three different haptic modeling components because the information provided by the friction, tapping response, and texture vibrations is processed together and may provide redundant cues. The study in [44], which tested the relative contribution of tactile and auditory information to judgments of roughness, overcame this problem by removing tactile and auditory information one at a time. The perceptual discrepancy between the two feedback components allowed subjects to disambiguate the relative contributions of the tactile and auditory information. We followed a similar perceptual discrepancy paradigm by turning the modeling components off one at a time. This study design created four virtually rendered surfaces for each real surface: the control surface displaying all components, one surface without friction, one surface without tapping transients, and one surface without texture vibrations.

The subject was simultaneously presented with one real surface and one of its four corresponding virtual surfaces.

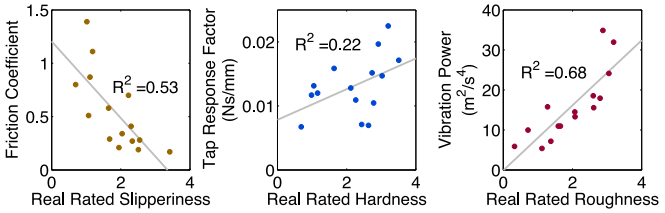

Fig. 6. Comparison of the measured surface parameters to the subjects' ratings of the 15 real surfaces along the three adjective scales. There is a high degree of correlation between the friction coefficient and the rated slipperiness, and between the acceleration power and the rated roughness. There is weak correlation between the tap response factor and the rated hardness.

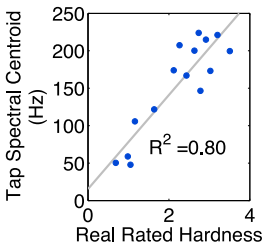

Fig. 7. Comparison of the tap spectral centroid to the subject's hardness ratings for the 15 real surfaces. The tap spectral centroid was found to be a better predictor of rated hardness than the tap response factor.

After exploring both surfaces, the subject was asked to rate the similarity between the two surfaces by placing a mark on a scale of "completely different" to "completely the same" on a computer using a mouse. The subject was required to tap on the virtual surface at least five times and drag along it for at least 50 cm before providing the rating. The real surfaces were presented in randomized order, and the four virtual surfaces were also presented in randomized order. The subject rated the similarity between a real surface and all four virtual versions of that real surface before moving on to the next real surface.

4.4 Collecting Physical Interaction Data

To fully interpret the results of our human-subject study, we need to analyze the forces and vibrations that the user is actually feeling. This comparison of the commanded haptic signals to the actual signals felt by the user allows us to better understand whether changes in realism stem from the haptic models or are artifacts of the rendering methods. To accomplish this comparison, we recorded force and vibration data from tapping and dragging on two representative surfaces (Brick 1 and MDF), as well as the base surface, which was displayed without friction, tapping transients, or texture vibrations.

To measure the friction force felt by the user, a six-axis force-torque sensor (ATI Industrial Automation Mini40 SI-40-2) was placed underneath the Omni. A ± 6 g three-axis accelerometer (STMicroelectronics LIS344ALH) was glued to the stylus of the Omni to measure the output tapping transients and texture vibrations. The data signals from the force sensor and the accelerometer were read into an analog-to-digital converter on a microcontroller (ATmega32u4) at 3 kHz. The commanded force and vibration signals were recorded using the OpenHaptics program at 1 kHz. The three vibration signals were mapped onto a single axis using the DFT321 algorithm [34]. To allow for direct comparison between the commanded and recorded signals, the commanded force and vibration signals were resampled at 3 kHz and the signals were aligned temporally.

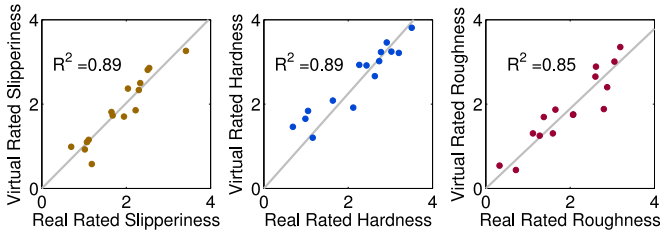

Fig. 8. Comparison of the subjects' ratings of the control virtual surfaces to their ratings of the 15 real surfaces along the three adjective scales along the same scale. There is high correlation between the rated characteristics of the real and virtual surfaces for all three perceptual dimensions.

5 Results

5.1 Adjective Ratings

The adjective ratings were normalized by dividing each rating by the standard deviation of all ratings given by that subject for that scale. The normalized adjective ratings were then averaged across all subjects.

Fig. 6 shows the correlation between the average adjective ratings and measured physical parameters calculated in Section 4.2. The average rated slipperiness was moderately inversely correlated with the measured friction coefficient ($R^2 = 0.53$, $p = 2.20 \times 10^{-3}$), and the average rated roughness was highly correlated with the acceleration power ($R^2 = 0.68$, $p = 1.57 \times 10^{-4}$). Although the tap response factor was used to characterize the 100 surfaces in the clustering analysis in Section 4.2, this measurement was found to have a lower than expected correlation with the rated hardness of the real surfaces ($R^2 = 0.22$, $p = 0.076$). Instead, we found the spectral centroid of the tapping transient vibrations had the best correlation with the average rated hardness ($R^2 = 0.80$, $p = 7.30 \times 10^{-6}$), as shown in Fig. 7. Following the work of [45], the average spectral centroid of each surface's tapping transients was calculated across several representative taps using the equation

$$\mathrm{SC} = \frac{\sum_k X(f_k)^2 f_k}{\sum_k X(f_k)^2}, \tag{4}$$

where $X(f_k)$ is the normalized amplitude of the DFT at frequency f_k. We chose a subset of incoming speeds that were commonly used by subjects when tapping on a virtual surface with the Omni. Tapping transients were calculated at every 10 mm/s in the interval from 50 mm/s to 100 mm/s; the spectral centroids of the resulting transients were calculated and averaged across all speeds.

There was a high degree of negative correlation between the ratings of roughness and slipperiness for real surfaces ($R = -0.91$, $p = 3.53 \times 10^{-6}$) and between the ratings of roughness and slipperiness for virtual surfaces ($R = -0.74$, $p = 0.002$). No other correlations were significant.

Fig. 8 shows the relationship between the rated adjectives for the corresponding real and virtual surfaces. All three sets of adjectives are highly correlated across the real and

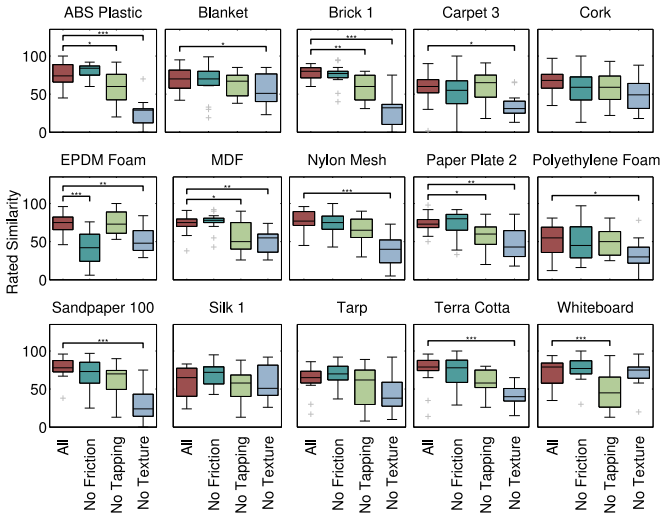

Fig. 9. Comparison of similarity ratings across the four virtual versions of each surface. Statistically significant differences in similarity from the control virtual surface are marked with a bar and asterisks ($*** \equiv p \leq 0.001$, $** \equiv p \leq 0.01$, $* \equiv p \leq 0.05$).

virtual surfaces including the slipperiness ($R^2 = 0.89$, $p = 1.55 \times 10^{-7}$), the hardness ($R^2 = 0.89$, $p = 1.56 \times 10^{-7}$), and the roughness ($R^2 = 0.85$, $p = 9.78 \times 10^{-7}$).

5.2 Similarity Ratings

Box plots of the four similarity ratings for each surface (Fig. 9) provide a visual representation of the relative importance of the three rendering components, which is different for each surface. A two-way analysis of variance (ANOVA) was performed for each surface on the similarity ratings with rendering condition and subject as the factors. A Tukey-Kramer multiple comparison test was conducted on the ANOVA results to determine which conditions, if any, had a significantly different mean from the control condition for each surface.

The similarity ratings between real and virtual surfaces decreased significantly for some conditions in which a rendering component was removed, whereas some other similarities showed no statistically significant difference if a component was removed. Removing the surface friction created a statistically significant decrease in real-virtual similarity for only one surface: EPDM Foam ($p = 1.26 \times 10^{-5}$). Removing the tapping transient response created a statistically significant decrease in similarity for five surfaces: ABS Plastic ($p = 0.036$), Brick 1 ($p = 0.004$), MDF ($p = 0.018$), Paper Plate 2 ($p = 0.042$), and Whiteboard ($p = 5.46 \times 10^{-4}$). Removing the texture vibrations created a statistically

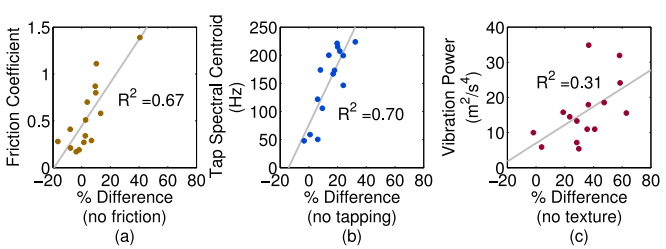

Fig. 10. Relationship between the surfaces' physical parameters and the percent difference in similarity ratings resulting from the removal of the relevant modeling component.

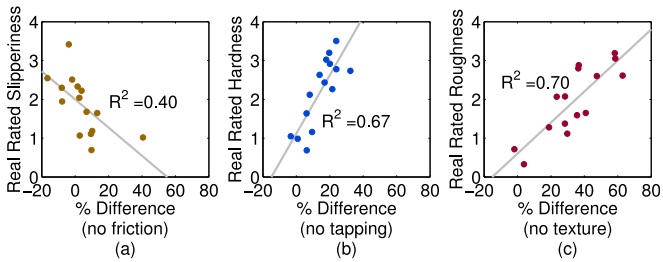

Fig. 11. Relationship between the average adjective ratings of the real surfaces and the percent difference in similarity ratings resulting from the removal of the relevant modeling component.

significant decrease in similarity for eleven surfaces: ABS Plastic ($p = 4.02 \times 10^{-9}$), Blanket ($p = 0.033$), Brick 1 ($p = 3.89 \times 10^{-9}$), Carpet 3 ($p = 0.033$), EPDM Foam ($p = 0.003$), MDF ($p = 0.001$), Nylon Mesh ($p = 4.22 \times 10^{-8}$), Paper Plate 2 ($p = 0.001$), Polyethylene Foam ($p = 0.027$), Sandpaper 100 ($p = 8.52 \times 10^{-8}$), and Terra Cotta ($p = 8.16 \times 10^{-5}$). None of the differences in real-virtual similarity ratings were significant for three surfaces: Cork, Silk 1, and Tarp. Subject was a significant factor for all surfaces.

For subsequent analyses, each subject's similarity ratings were normalized by the standard deviation of their ratings to compensate for individual differences in subjective rating scales. The normalized similarity ratings were then averaged across all subjects.

To determine how the similarity ratings change when the components are turned off one at a time, we first looked at the change in similarity rating as a function of the surface's measured parameters, as shown in Fig. 10. The percent differences were calculated as follows:

$$\%\text{diff}_x = \frac{S_1 - S_x}{S_1}, \tag{5}$$

where S_1 is the average normalized similarity rating when all model components were displayed and S_x is the average normalized similarity rating when the component of interest was removed. The measured friction coefficient was found to highly correlate to the percent difference in the similarity ratings when the friction was turned off ($R^2 = 0.67$, $p = 1.95 \times 10^{-4}$). The tapping spectral centroid was highly correlated with the percent difference in the similarity ratings when the tapping transients were turned off ($R^2 = 0.70$, $p = 1.12 \times 10^{-4}$). There was a weak correlation between the acceleration power and the percent difference between the similarity ratings when the texture vibrations were turned off ($R^2 = 0.31$, $p = 0.03$).

Lastly we looked at the change in similarity rating as a function of the adjective ratings of the real surfaces, as shown in Fig. 11. The percent differences were calculated as in Eq. (5). There was a weak inverse correlation between the average rated slipperiness and the percent difference between the similarity ratings when the friction was turned off ($R^2 = 0.40$, $p = 0.01$). The average rated hardness was highly correlated with the percent difference in the similarity ratings when the tapping transients were turned off ($R^2 = 0.67$, $p = 1.94 \times 10^{-4}$). The average rated roughness was found to highly correlate with the percent difference in the similarity ratings when the texture vibrations were turned off ($R^2 = 0.70$, $p = 9.39 \times 10^{-5}$).

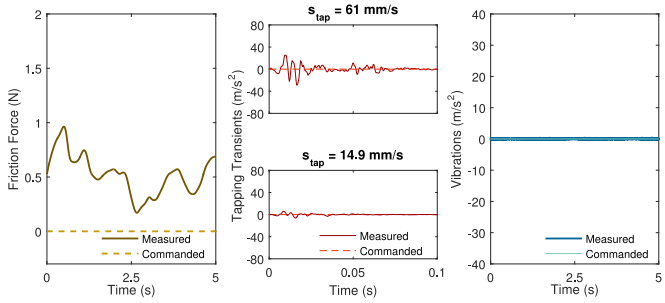

Fig. 12. Commanded and measured forces and vibrations recorded from tapping and dragging on a base virtual surface. The commanded friction, tapping transients, and texture vibrations are set to zero.

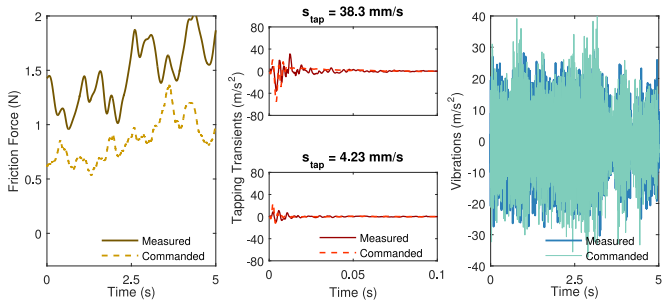

Fig. 13. Commanded and measured forces and vibrations recorded from tapping and dragging on the virtual Brick 1 surface.

5.3 Physical Interaction Data

Fig. 12 shows force and acceleration data that were recorded when the experimenter was interacting with a base virtual surface in which the friction, tapping transients, and texture vibrations were set to zero. Even though the surface was displayed without friction, the user felt a noticeable friction force of about 0.6 N when dragging across the virtual surface. This friction force, which is caused by the internal mechanics of the Omni, was not consistently related to the user's applied normal force, and it depended on the position in the Omni's workspace. Transient vibrations were measured as the user tapped on the virtual surface. Although no tapping transients were commanded, the measured vibrations that were observed depend on speed, which is similar to tapping transients from physical surfaces. During dragging, no texture vibrations were displayed, but vibrations that were caused by the Omni's internal mechanisms were measured ($P_{\text{avg}} = 0.15\,\text{m}^2/\text{s}^4$).

Fig. 13 shows force and acceleration data that were recorded from interacting with the virtual Brick surface. During dragging, the measured friction force was on average 0.6 N greater than the commanded friction force. The measured tapping transients had higher frequency content than the commanded tapping transients and tended to damp out more slowly, which is more noticeable in the tap at higher speed. The average power of the measured texture vibrations ($P_{\text{meas}} = 85.7\,\text{m}^2/\text{s}^4$) is slightly higher than the average power of the commanded texture vibrations ($P_{\text{com}} = 81.4\,\text{m}^2/\text{s}^4$), relative to the signals' average power ($p_{\text{diff}} = 5.2\%$).

Fig. 14 shows force and acceleration data that were recorded from interacting with a virtual MDF surface. During dragging, the measured friction force was on average 0.7 N greater than the commanded friction force. Similar to

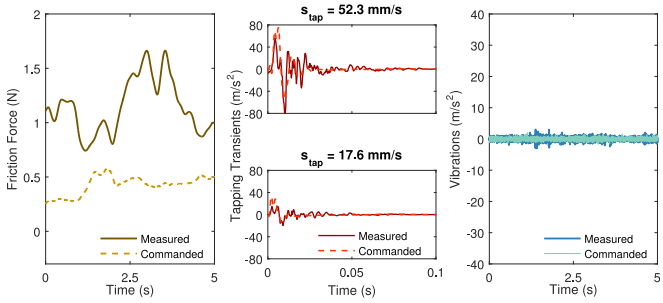

Fig. 14. Commanded and measured forces and vibrations recorded from tapping and dragging on the virtual MDF surface.

the data from Brick 1, the measured tapping transients had higher frequency content than the commanded tapping transients and tended to damp out more slowly, especially at the higher tap speed. The average power of the measured texture vibrations ($P_{\text{meas}} = 0.39\,\text{m}^2/\text{s}^4$) is considerably higher than the average power of the commanded texture vibrations ($P_{\text{com}} = 0.22\,\text{m}^2/\text{s}^4$), relative to the signals' average power ($p_{\text{diff}} = 55.7\%$).

6 Discussion

By evaluating how the similarity between real and virtual surfaces changes upon removal of individual model components, the study provided valuable insights into the strengths of our modeling approach and the importance of the perceptual dimensions (slipperiness, hardness, and roughness) to the realism of haptic virtual surfaces. The high correlation between the real and virtual adjective ratings for all three scales (Fig. 8) indicates that the modeling and rendering methods presented in this paper capture all three perceptual dimensions. This correlation shows a marked improvement over the rendering methods presented in [13], which accurately captured only the roughness of the surfaces by displaying the texture vibrations. Using all three surface model components accurately captures the three perceptual dimensions of surface interactions with a tool.

However, Fig. 9 showed that the rendering components are not equally important to the real-virtual similarity of all surfaces. A cursory glance shows that displaying the texture vibrations appears to be the most important because removing texture vibrations creates a statistically significant decrease in similarity for the largest number of surfaces. However, removing the texture vibrations did not result in a significant change in similarity for four surfaces. Furthermore, removing the friction or tapping transients creates a significant decrease in similarity rating for some surfaces, indicating that the importance of the separate modeling components is complex. As suggested by Fig. 10, the relative difference in similarity ratings depends on the physical parameters of the surface.

6.1 Slipperiness

The percent difference in similarity rating when friction is removed significantly correlates with the measured friction coefficient, as shown in Fig. 10a. In simple terms, rendering friction is more important for surfaces with high friction. Interestingly, the similarity ratings for surfaces with the

lowest coefficients of friction (Whiteboard: $\mu_k = 0.17$, MDF: $\mu_k = 0.19$, ABS Plastic: $\mu_k = 0.21$, Silk 1: $\mu_k = 0.28$, and Tarp: $\mu_k = 0.41$) improve when friction is removed. This negative percent difference suggests that the friction of these virtual surfaces was too high. One reason for this discrepancy is the presence of friction in the motors and joints of the Omni, which was not taken into account when rendering the surfaces. This undesired friction, which is shown in Fig. 12, adds to the commanded friction so that the user feels a friction force that is much higher than desired, as shown in Figs. 13 and 14. Thus, when the modeled surface friction was added to the Omni's internal friction, the subjects perceived the surface friction as being too high. This finding highlights the need to take the frictional properties of the device into consideration when rendering virtual surfaces.

Realism could be further improved by adjusting the surface friction model. As described in Section 3, the value of $z_{\max}$, which determines the transition between sticking and sliding, was set to be proportional to the kinetic friction coefficient to ensure stability, but this choice does not follow the physical behavior of the system. This heuristic model parameter resulted in unrealistic static friction, which probably affected the perceived slipperiness of the virtual surfaces. The friction model could be improved by fitting this parameter using the recorded data, as was done in [20] by modeling additional friction behavior.

Although Fig. 6 shows that the real ratings of slipperiness are moderately correlated with the physical measurements of surface friction, they show only weak correlation to the percent difference in similarity ratings when the surface friction was removed (Fig. 11a). This discrepancy indicates that friction is not the only contributor to the perceived slipperiness of the surface. This observation is supported by the high correlation seen between the real ratings of roughness and slipperiness and between the virtual ratings of roughness and slipperiness. Thus, the surface roughness, and consequently the texture vibrations, likely play a role in the perceived slipperiness of a surface. This phenomenon was also uncovered by the human experiment results in [13] and has been studied in [25]. Thus, to fully capture the slipperiness of a surface, both the surface friction and the texture vibrations must be displayed on the virtual surface.

6.2 Hardness

Contrary to our assumption in Section 4.2, this study found that the tap response factor proposed in [41] was not a strong indicator of rated hardness. Rather, the spectral centroid of the tapping transient vibrations was the best predictor of perceptual hardness ratings (Fig. 7). The relationship between spectral centroid and hardness results from differences in physical properties of the tool-hand-surface system for hard and soft surfaces. As discussed in [46], impact with high stiffness surfaces elicits wide-bandwidth transient vibrations, and impact with low stiffness surfaces elicits lower-bandwidth vibrations that are damped out quickly. Therefore, the tapping transient vibrations for hard surfaces will have a higher spectral centroid than tapping transient vibrations for soft surfaces. These trends can be observed in the DFTs shown in Fig. 2. Conversely, the tap response factor ignores the essential information in the spectra of the taps, which resulted in the poor correlation shown in Fig. 6.

The percent difference in similarity rating when the tapping transients are removed is significantly correlated with the measured tapping spectral centroid (Fig. 10b) and the rated hardness (Fig. 11b). Only one surface had a negative percent difference: Carpet 3. Since this surface had the lowest tap spectral centroid ($SC_{\text{tap}} = 47.8$ Hz), it was physically the softest of the tested surfaces. The negative percent difference indicates that virtual Carpet 3 was perceived as too hard, which may have been because the underlying stiffness of the surface was too high. All virtual surfaces were rendered using the same underlying stiffness (0.25 N/mm); however, the underlying base surface contributes additional tapping transients, as shown in Fig. 12. These undesired transients were not taken into account when displaying the tapping transients for the virtual surfaces, which resulted in the user feeling higher amplitude transients than desired. Displaying tapping transients can make a virtual surface feel harder, but they may not needed for very soft surfaces that can simply be rendered using Hooke's law.

Furthermore, the ability of the Omni to accurately display the tapping transients was not considered during rendering; Figs. 13 and 14 showed that the transients felt by the user had higher frequency content and damped out more slowly. Contrary to this work, which simply scaled the tapping transient acceleration to display them as a force, other work characterized the output device to determine the force profile needed to produce a desired acceleration signal [4]. This careful acceleration matching is needed to accurately reproduce the desired transients and should be implemented when high fidelity renderings are required.

Inconsistencies in the friction model also may have affected the perceived hardness of the surfaces. Since the value of $z_{\max}$ was heuristically chosen, the amount of deformation of the virtual surface in the pre-sliding condition did not match that of the physical surface. This resulted in a virtual surface that may have felt either harder or softer than its real counterpart.

6.3 Roughness

The percent difference in similarity ratings when the texture vibrations were removed was strongly correlated to the rated roughness of the real surfaces (Fig. 11c), which supports the conclusions of previous work that the roughness information is encoded in the vibrations [23], [24], [25], [26]. Furthermore, the real roughness ratings were correlated with the acceleration power (Fig. 6), which shows that the power of the vibrations is important in determining roughness. However, the percent difference in similarity rating when the texture vibrations were removed is only weakly correlated to the acceleration power, as shown in Fig. 10c. This disparity indicates that the power was not the only important component of the vibration signal; subjects were probably also paying attention to the signal's spectral properties. Therefore, to display the roughness of a surface, it is necessary to model and render the texture vibrations. For very smooth surfaces, however, displaying texture vibrations may not be needed to create a realistic virtual surface.

A further compounding factor is the level of vibrations introduced through the internal mechanisms of the Omni. These undesired vibrations are added to the vibrations played through the Haptuator, so that the user feels vibrations that are stronger than those commanded. This difference disproportionately affects the feel of smoother surfaces that have lower power texture vibrations because the undesired vibrations can dominate and overpower what the user feels, as shown in Fig. 14. For rougher surfaces, however, these additional vibrations only marginally affect what the user feels, as shown in Fig. 13.

The results of this study show that the importance of rendering the surface friction, tapping transients, or texture vibrations depends on the physical surface being modeled. When deciding whether to include a rendering component or not, researchers should balance the potential increase in realism with the computational and hardware costs of adding that component. To further increase realism, researchers should also take into account the mechanical properties of the rendering hardware, such as friction and frequency response, when displaying the modeled components to the user.

7 Conclusion

This article evaluated methods for modeling and rendering haptic virtual surfaces from data recorded during tool-surface interactions. The virtual surfaces were created using a combination of friction, tapping transient, and texture vibration models to capture the full haptic experience, and they were rendered using an Omni force-feedback device augmented with a Haptuator. We summarized the data recording, modeling, and rendering steps for the three component models, which were developed in prior work. A Coulomb friction relationship was fit to data recorded from dragging on the surface and was rendered using a stick-slip Dahl friction model. The tapping vibration transients were modeled from data recorded during tapping on the physical surfaces at various speeds. During rendering, the tapping transients are displayed as momentum-cancelling force transients. Piecewise autoregressive texture models were created to represent the vibrations induced in a tool as it is dragged across a textured surface. A synthetic vibration signal is generated and displayed through a voice-coil actuator attached to the tip of the Omni.

We ran a study that evaluated the decrease in similarity between real and virtual surfaces created by the removal of friction, tapping, and texture cues. Subjects rated real and virtual surfaces along three adjective scales (slipperiness, hardness, and roughness), and subjects also rated the similarity between pairs of real and virtual surfaces. Four virtual surfaces were created for each real surface: one control surface in which all model components were displayed and three surfaces in which the model components were turned off one at a time. The study indicated that the combination of surface friction, tapping transient, and texture vibration models fully captured the surfaces' slipperiness, hardness, and roughness. However, the importance of the three model components was not constant across surfaces. We found that the importance of the three separate modeling components had an approximately linear relationship with the physical parameters and the adjective ratings of the real surfaces. Intuitively, rendering a given component of a surface is important when that surface property is strong.

We further analyzed the forces and vibrations felt by the user to determine the fidelity of the rendering system in displaying the desired haptic signals. Our analysis indicated that the friction forces, tapping transients, and texture vibrations were negatively affected by the Omni's mechanical properties. To further increase realism, the mechanics of the rendering hardware must be accounted for so the user feels an undistorted version of the commanded signals. Researchers can use the results of the reported study to decide whether to include friction, tapping, and/or texture in their haptic applications.

Acknowledgments

The authors thank Juan José López Delgado for his work in creating the Penn Haptic Texture Toolkit. This work was supported by the US National Science Foundation under Grant No. 0845670. Heather Culbertson was also supported by a research fellowship from the US National Science Foundation Graduate Research Fellowship Program under Grant No. DGE-0822.

References

[1] R. H. LaMotte, "Softness discrimination with a tool," *J. Neurophysiology*, vol. 83, no. 4, pp. 1777–1786, 2000.

[2] R. L. Klatzky, S. J. Lederman, C. Hamilton, M. Grindley, and R. H. Swendsen, "Feeling textures through a probe: Effects of probe and surface geometry and exploratory factors," *Attention, Perception Psychophysics*, vol. 65, no. 4, pp. 613–631, 2003.

[3] G. Campion and V. Hayward, "Fundamental limits in the rendering of virtual haptic textures," in *Proc. IEEE World Haptics Conf.*, 2005, pp. 263–270.

[4] K. J. Kuchenbecker, J. P. Fiene, and G. Niemeyer, "Improving contact realism through event-based haptic feedback," *IEEE Trans. Vis. Comput. Graph.*, vol. 12, no. 2, pp. 219–230, Mar./Apr. 2006.

[5] N. Diolaiti, G. Niemeyer, F. Barbagli, and J. K. Salisbury, "Stability of haptic rendering: Discretization, quantization, time delay, and coulomb effects," *IEEE Trans. Robotics*, vol. 22, no. 2, pp. 256–268, Apr. 2006.

[6] M. C. Çavuşoğlu, D. Feygin, and F. Tendick, "A critical study of the mechanical and electrical properties of the Phantom haptic interface and improvements for high performance control," *Presence: Teleoperators Virtual Environments*, vol. 11, no. 6, pp. 555–568, 2002.

[7] M. A. Otaduy and M. C. Lin, "Rendering of textured objects," in *Haptic Rendering: Foundations, Algorithms, and Applications*, M. Lin and M. Otaduy, Eds. Natick, MA, USA: AK Peters, 2008, ch. 18, pp. 371–393.

[8] C. McDonald and K. J. Kuchenbecker, "Dynamic simulation of tool-mediated texture interaction," in *Proc. IEEE World Haptics Conf.*, Apr. 2013, pp. 307–312.

[9] A. M. Okamura, K. J. Kuchenbecker, and M. Mahvash, "Measurement-based modeling for haptic display," in *Haptic Rendering: Foundations, Algorithms, and Applications*, M. Lin and M. Otaduy, Eds. Natick, MA, USA: AK Peters, 2008, ch. 21, pp. 443–467.

[10] J. M. Romano and K. J. Kuchenbecker, "Creating realistic virtual textures from contact acceleration data," *IEEE Trans. Haptics*, vol. 5, no. 2, pp. 109–119, Apr.–Jun. 2012.

[11] H. Culbertson, J. M. Romano, P. Castillo, M. Mintz, and K. J. Kuchenbecker, "Refined methods for creating realistic haptic virtual textures from tool-mediated contact acceleration data," in *Proc. IEEE Haptics Symp.*, Mar. 2012, pp. 385–391.

[12] H. Culbertson, J. Unwin, B. E. Goodman, and K. J. Kuchenbecker, "Generating haptic texture models from unconstrained tool-surface interactions," in *Proc. IEEE World Haptics Conf.*, Apr. 2013, pp. 295–300.

[13] H. Culbertson, J. Unwin, and K. J. Kuchenbecker, "Modeling and rendering realistic textures from unconstrained tool-surface interactions," *IEEE Trans. Haptics*, vol. 7, no. 3, pp. 381–393, Jul.–Sep. 2014.

[14] H. Culbertson, J. J. López Delgado, and K. J. Kuchenbecker, "One hundred data-driven haptic texture models and open-source methods for rendering on 3D objects," in *Proc. IEEE Haptics Symp.*, Feb. 2014, pp. 319–325.
[15] S. Okamoto, H. Nagano, and Y. Yamada, "Psychophysical dimensions of tactile perception of textures," *IEEE Trans. Haptics*, vol. 6, no. 1, pp. 81–93, Jan.–Mar. 2012.
[16] T. Yamauchi, S. Okamoto, M. Konyo, Y. Hidaka, T. Maeno, and S. Tadokoro, "Real-time remote transmission of multiple tactile properties through master-slave robot system," in *Proc. IEEE Int. Conf. Robotics Autom.*, 2010, pp. 1753–1760.
[17] W. McMahan, J. M. Romano, A. M. Abdul Rahuman, and K. J. Kuchenbecker, "High frequency acceleration feedback significantly increases the realism of haptically rendered textured surfaces," in *Proc. IEEE Haptics Symp.*, 2010, pp. 141–148.
[18] C. Richard, M. R. Cutkosky, and K. MacLean, "Friction identification for haptic display," in *Proc. ASME Dynamic Syst. Control Division*, 1999, vol. 67, pp. 327–334.
[19] K. Worden, et al., "Identification of pre-sliding and sliding friction dynamics: Grey box and black-box models," *Mech. Syst. Signal Process.*, vol. 21, no. 1, pp. 514–534, 2007.
[20] S. Jeon, J.-C. Metzger, S. Choi, and M. Harders, "Extensions to haptic augmented reality: Modulating friction and weight," in *Proc. IEEE World Haptics Conf.*, 2011, pp. 227–232.
[21] P. Wellman and R. D. Howe, "Towards realistic vibrotactile display in virtual environments," *Proc. ASME Dynamic Syst. Control Division*, vol. 57, no. 2, pp. 713–718, 1995.
[22] A. M. Okamura, J. T. Dennerlein, and R. D. Howe, "Vibration feedback models for virtual environments," in *Proc. IEEE Int. Conf. Robotics Autom.*, May 1998, pp. 674–679.
[23] R. L. Klatzky and S. J. Lederman, "Tactile roughness perception with a rigid link interposed between skin and surface," *Perception Psychophysics*, vol. 61, no. 4, pp. 591–607, 1999.
[24] S. J. Bensmaïa and M. Hollins, "The vibrations of texture," *Somatosensory Motor Res.*, vol. 20, no. 1, pp. 33–43, 2003.
[25] W. M. Bergmann Tiest and A. M. Kappers, "Haptic and visual perception of roughness," *Acta Psychologica*, vol. 124, no. 2, pp. 177–189, 2007.
[26] T. Yoshioka, S. Bensmaia, J. Craig, and S. Hsiao, "Texture perception through direct and indirect touch: An analysis of perceptual space for tactile textures in two modes of exploration," *Somatosensory Motor Res.*, vol. 24, no. 1/2, pp. 53–70, 2007.
[27] V. L. Guruswamy, J. Lang, and W. S. Lee, "Modeling of haptic vibration textures with infinite-impulse-response filters," in *Proc. IEEE Int. Workshop Haptic Audio Visual Environments Games*, Nov. 2009, pp. 105–110.
[28] J. Lang and S. Andrews, "Measurement-based modeling of contact forces and textures for haptic rendering," *IEEE Trans. Vis. Comput. Graph.*, vol. 17, no. 3, pp. 380–391, Mar. 2011.
[29] J. M. Romano, T. Yoshioka, and K. J. Kuchenbecker, "Automatic filter design for synthesis of haptic textures from recorded acceleration data," in *Proc. IEEE Int. Conf. Robotics Autom.*, May 2010, pp. 1815–1821.
[30] Y. Takeuchi, S. Kamuro, K. Minamizawa, and S. Tachi, "Haptic duplicator," in *Proc. ACM Virtual Reality Int. Conf.*, 2012, pp. 30:1–30:2.
[31] S. Saga and R. Raskar, "Simultaneous geometry and texture display based on lateral force for touchscreen," in *Proc. SIGGRAPH Asia Emerging Technol.*, 2012, pp. 8:1–8:3.
[32] H. Culbertson and K. J. Kuchenbecker, "Should haptic texture vibrations respond to user force and speed?" in *Proc. IEEE World Haptics Conf.*, Jun. 2015, pp. 106–112.
[33] V. Hayward and B. Armstrong, "A new computational model of friction applied to haptic rendering," in *Experimental Robotics VI*. Berlin, Germany: Springer, 2000, pp. 403–412.
[34] N. Landin, J. M. Romano, W. McMahan, and K. J. Kuchenbecker, "Dimensional reduction of high-frequency accelerations for haptic rendering," in *Haptics: Generating and Perceiving Tangible Sensations*, A. Kappers, J. van Erp, W. Bergmann Tiest, and F. van der Helm, Eds. Berlin, Germany: Springer, Jul. 2010, pp. 79–86.
[35] J. Bell, S. Bolanowski, and M. Holmes, "The structure and function of Pacinian corpuscles: A review," *Progress Neurobiology*, vol. 42, no. 1, pp. 79–128, 1994.
[36] M. A. Srinivasan and C. Basdogan, "Haptics in virtual environments: Taxonomy, research status, and challenges," *Comput. Graph.*, vol. 21, no. 4, pp. 393–404, 1997.
[37] H. Culbertson, J. J. Lopez Delgado, and K. J. Kuchenbecker, "The Penn Haptic Texture Toolkit for modeling, rendering, and evaluating haptic virtual textures," Feb. 2014. [Online]. Available: http://repository.upenn.edu/meam_papers/299/
[38] P. R. Dahl, "A solid friction model," Aerospace Corp., El Segundo, CA, Tech. Rep. TOR-0158(3107–18)-1, 1968.
[39] G. Box and G. Jenkins, *Time Series Analysis: Forecasting and Control*. San Francisco, CA, USA: Holden-Day, 1970.
[40] S. J. Lederman and S. G. Abbott, "Texture perception: Studies of intersensory organization using a discrepancy paradigm, and visual versus tactual psychophysics," *J. Exp. Psychology: Human Perception Performance*, vol. EP-7, no. 4, 1981, Art. no. 902.
[41] J. P. Fiene and K. J. Kuchenbecker, "Shaping event-based haptic transients via an improved understanding of real contact dynamics," in *Proc. IEEE World Haptics Conf.*, 2007, pp. 170–175.
[42] W. M. Bergmann Tiest, "Tactual perception of material properties," *Vision Res.*, vol. 50, no. 24, pp. 2775–2782, 2010.
[43] P. A. Harris, R. Taylor, R. Thielke, J. Payne, N. Gonzalez, and J. G. Conde, "Research electronic data capture (REDCap)-a metadata-driven methodology and workflow process for providing translational research informatics support," *J. Biomed. Inform.*, vol. 42, no. 2, 2009, Art. no. 377.
[44] S. J. Lederman, R. L. Klatzky, T. Morgan, and C. Hamilton, "Integrating multimodal information about surface texture via a probe: Relative contributions of haptic and touch-produced sound sources," in *Proc. IEEE Haptics Symp.*, 2002, pp. 97–104.
[45] J. Fishel and G. Loeb, "Bayesian exploration for intelligent identification of textures," *Frontiers Neurorobotics*, vol. 6, 2012, Art. no. 4.
[46] Y. Visell and S. Okamoto, "Vibrotactile sensation and softness perception," in *Multisensory Softness*, M. D. Luca, Ed. Berlin, Germany: Springer, 2014, ch. 3, pp. 31–47.

Heather Culbertson received the BS degree in mechanical engineering from the University of Nevada, Reno, in 2010, and the master's degree from the Department of Mechanical Engineering and Applied Mechanics (MEAM), University of Pennsylvania, in May 2013. She also received the PhD degree from the Department of Mechanical Engineering and Applied Mechanics, University of Pennsylvania, in 2015 where she worked in the Haptics Group, a part of the GRASP Laboratory. She is a postdoctoral fellow of mechanical engineering with Stanford University. She is a member of the IEEE.

Katherine J. Kuchenbecker received the BS, MS, and PhD degrees in mechanical engineering from Stanford University, in 2000, 2002, and 2006, respectively. She completed a postdoctoral research fellowship at Johns Hopkins University, from 2006 to 2007. She is currently an associate professor of mechanical engineering and applied mechanics with the University of Pennsylvania. Her research centers on the design and control of haptic interfaces and robotic systems, and she directs the Penn Haptics Group, which is part of the General Robotics, Automation, Sensing, and Perception (GRASP) Laboratory. She was the recipient of the 2009 National Science Foundation CAREER Award, the 2008 and 2011 Citations for Meritorious Service as a reviewer for the *IEEE Transactions on Haptics*, and the 2012 IEEE Robotics and Automation Society Academic Early Career Award. She is co-chairing the IEEE Haptics Symposium in 2016 and 2018, and she is presently a co-chair of the IEEE RAS Technical Committee on Haptics. She is a member of the IEEE.